A

Day	Trial 1	Trial 2	Trial 3	Trial 4
1	E	S	SW	NE
2	SW	E	NE	S
3	NE	SW	S	E
4	S	NE	E	SW
5	E	SW	S	NE
6	SW	NE	E	S
7	NE	S	SW	E
8 (Probe)	SE			

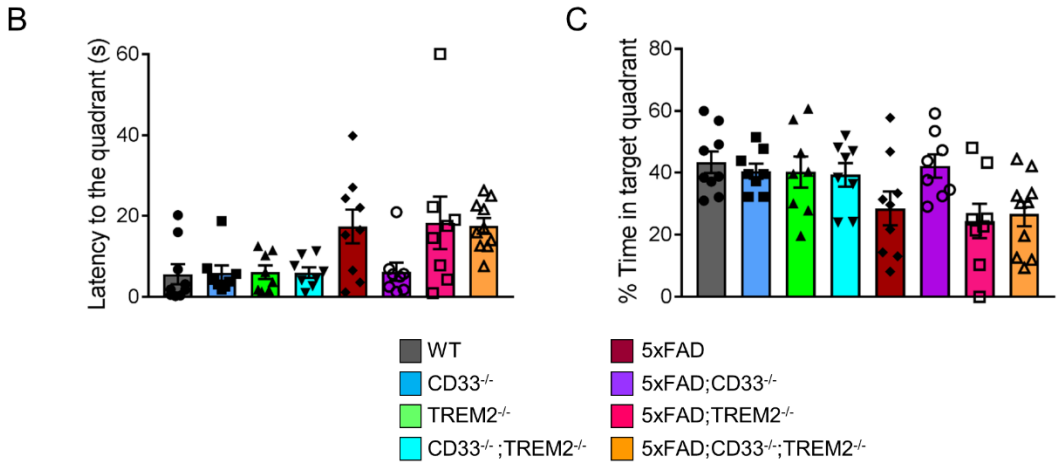

Figure S1. Morris water maze analysis, Related to Figure 1. (A) Start positions using distal locations for which the target (platform) was located in the North-West (NW) quadrant. (B and C) 7-month-old WT (n=5M/4F), *CD33*$^{-/-}$ (n=4M/4F), *TREM2*$^{-/-}$ (n=4M/4F), *CD33*$^{-/-}$*;TREM2*$^{-/-}$ (n=4M/4F), *5xFAD* (n=5M/4F), *5xFAD;CD33*$^{-/-}$ (n=4M/4F), *5xFAD;TREM2*$^{-/-}$ (n=4M/4F) and *5xFAD;CD33*$^{-/-}$*;TREM2*$^{-/-}$ (n=5M/5F) mice were evaluated in the Morris water maze test. Latency to reach the target quadrant where the platform is supposed to be (B) and time spent by the mice in the target quadrant (C) were recorded during the probe test (day 8). No significant differences were found among the mouse groups in the latency to the target quadrant (Kruskal-Wallis ANOVA, Dunn's test) or time spent in the target quadrant (one-way ANOVA, Tukey's test). Data are represented as mean ± SEM.

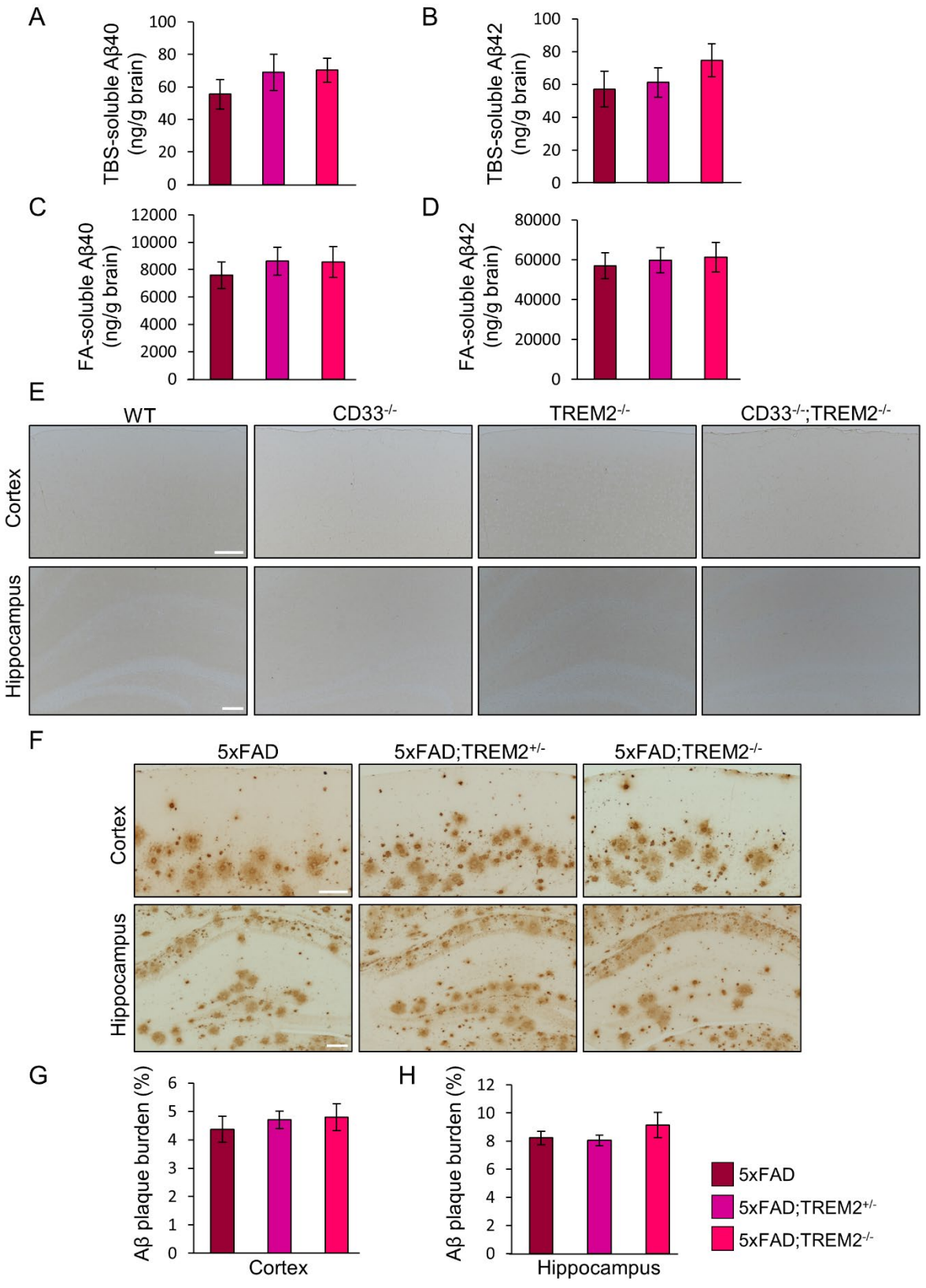
A
TBS-soluble Aβ40 (ng/g brain)
100
80
60
40
20
0
B
TBS-soluble Aβ42 (ng/g brain)
100
80
60
40
20
0
C
FA-soluble Aβ40 (ng/g brain)
12000
10000
8000
6000
4000
2000
0
D
FA-soluble Aβ42 (ng/g brain)
80000
60000
40000
20000
0
E
WT
CD33-/-
TREM2-/-
CD33-/-;TREM2-/-
Cortex
Hippocampus
F
5xFAD
5xFAD;TREM2+/-
5xFAD;TREM2-/-
Cortex
Hippocampus
G
Aβ plaque burden (%)
6
5
4
3
2
1
0
Cortex
H
Aβ plaque burden (%)
12
10
8
6
4
2
0
Hippocampus
5xFAD
5xFAD;TREM2+/-
5xFAD;TREM2-/-

Figure S2. *TREM2* knock-out does not impact Aβ pathology in *5xFAD* mice at 6 months of age, Related to Figure 2. (A–D) ELISA analysis of Aβ40 (A and C) and Aβ42 (B and D) in TBS-soluble (A and B) and formic acid (FA)-soluble (C and D) fractions isolated from the cortex of 6-month-old *5xFAD* (n=6M/6F), *5xFAD;TREM2*$^{+/-}$ (n=6M/6F) and *5xFAD;TREM2*$^{-/-}$ (n=4M/4F) mice. No differences in TBS- and FA-soluble Aβ40 and Aβ42 levels were found in *5xFAD;TREM2*$^{+/-}$ and *5xFAD;TREM2*$^{-/-}$ mice in comparison to *5xFAD* (one-way ANOVA, Tukey's test). (E) Brain sections were labeled with the 3D6 antibody directed against Aβ. Representative images of cortex and hippocampus from of 8-month-old control: WT, *CD33*$^{-/-}$, *TREM2*$^{-/-}$ and *CD33*$^{-/-}$*;TREM2*$^{-/-}$ mice. The 3D6 antibody did not label control brains. Scale bar represents 100 μm. (F) Photomicrographs of cortical and hippocampal fields from brains stained with the 3D6 antibody to detect compact and diffuse Aβ plaques in 6-month-old *5xFAD*, *5xFAD;TREM2*$^{+/-}$ and *5xFAD;TREM2*$^{-/-}$ mice. Scale bar represents 100 μm. (G and H) Quantification of Aβ plaque burden in the cortex (G) and hippocampus (H) of 6-month-old *5xFAD* (n=6M/6F), *5xFAD;TREM2*$^{+/-}$ (n=6M/6F) and *5xFAD;TREM2*$^{-/-}$ (n=4M/4F) mice. There was no significant difference in Aβ plaque load in *5xFAD;TREM2*$^{+/-}$ and *5xFAD;TREM2*$^{-/-}$ mice compared to *5xFAD* (one-way ANOVA, Tukey's test). Data are represented as mean ± SEM.

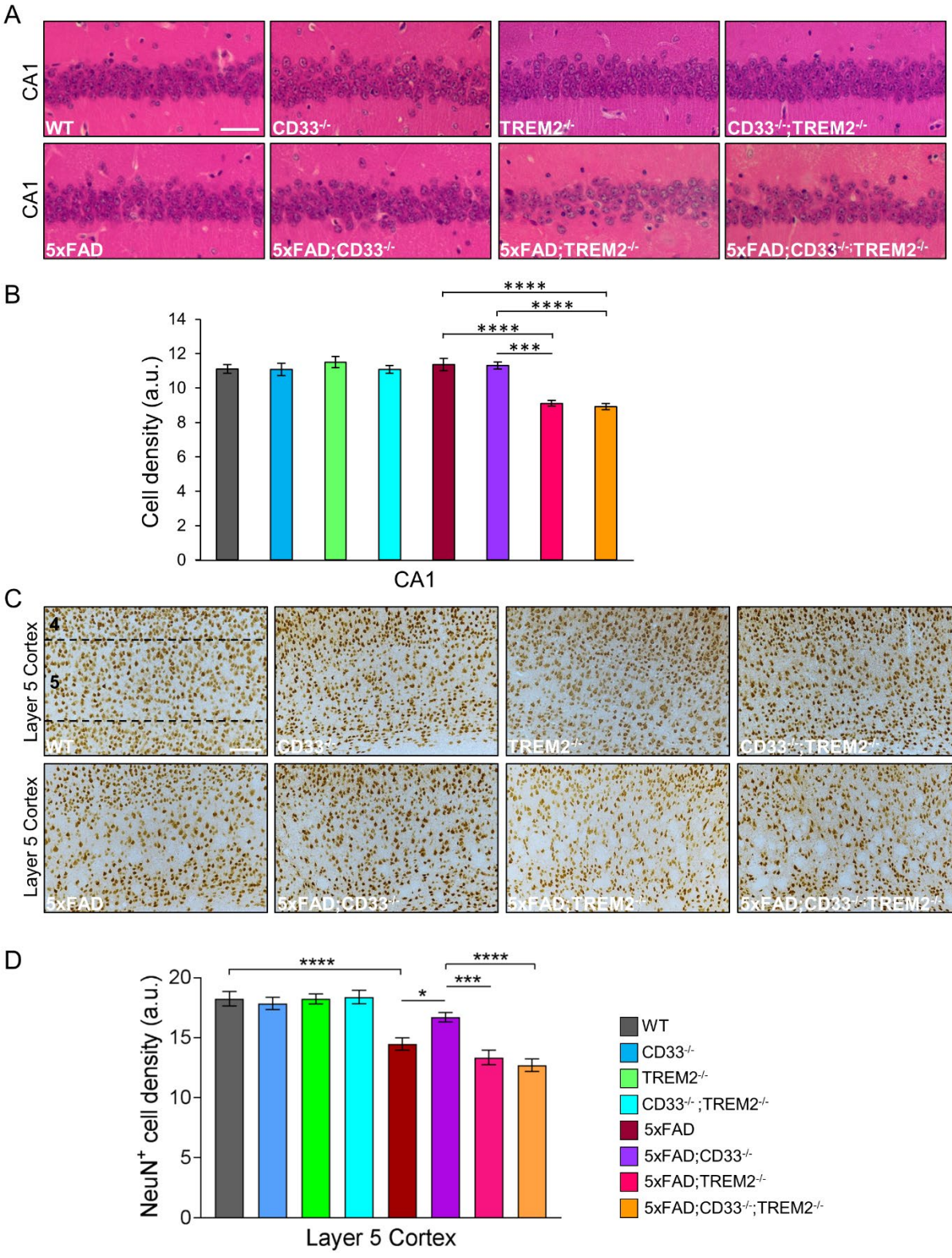
A
CA1
WT
CD33-/-
TREM2-/-
CD33-/-;TREM2-/-
CA1
5xFAD
5xFAD;CD33-/-
5xFAD;TREM2-/-
5xFAD;CD33-/-;TREM2-/-
B
Cell density (a.u.)
CA1
****
****
****
***
C
Layer 5 Cortex
4
5
WT
CD33-/-
TREM2-/-
CD33-/-;TREM2-/-
Layer 5 Cortex
5xFAD
5xFAD;CD33-/-
5xFAD;TREM2-/-
5xFAD;CD33-/-;TREM2-/-
D
NeuN+ cell density (a.u.)
Layer 5 Cortex
****
*
***
****
WT
CD33-/-
TREM2-/-
CD33-/- ;TREM2-/-
5xFAD
5xFAD;CD33-/-
5xFAD;TREM2-/-
5xFAD;CD33-/-;TREM2-/-

Figure S3. *TREM2* knock-out leads to reduced neuronal cell density in *5xFAD* mice, which is not rescued by additional knock-out of *CD33*, Related to Figure 3. (A) Representative pictures of the CA1 region from brains of 8-month-old mice of indicated genotypes, stained with hematoxylin and eosin. Scale bar represents 50 µm. (B) Quantification of CA1 neuron numbers in 8-month-old WT (n=6M/6F), *CD33*$^{-/-}$ (n=4M/4F), *TREM2*$^{-/-}$ (n=4M/4F), *CD33*$^{-/-}$*;TREM2*$^{-/-}$ (n=4M/4F), *5xFAD* (n=5M/6F), *5xFAD;CD33*$^{-/-}$ (n=4M/4F), *5xFAD;TREM2*$^{-/-}$ (n=4M/4F) and *5xFAD;CD33*$^{-/-}$*;TREM2*$^{-/-}$ (n=5M/6F) mice. *5xFAD;TREM2*$^{-/-}$ and *5xFAD;CD33*$^{-/-}$*;TREM2*$^{-/-}$ mice showed reduced CA1 neuronal cell density in comparison to *5xFAD* and *5xFAD;CD33*$^{-/-}$ mice (***p<0.001, ****p<0.0001, one-way ANOVA, Tukey's test). (C) Representative images from the cortex of 8-month-old mice of indicated genotypes, labeled with a NeuN-specific antibody. Scale bar represents 100 µm. (D) Quantification of NeuN^{+} cells in the cortical layer 5 of 8-month-old WT (n=4M/4F), *CD33*$^{-/-}$ (n=4M/4F), *TREM2*$^{-/-}$ (n=4M/4F), *CD33*$^{-/-}$*;TREM2*$^{-/-}$ (n=4M/4F), *5xFAD* (n=7M/7F), *5xFAD;CD33*$^{-/-}$ (n=7M/7F), *5xFAD;TREM2*$^{-/-}$ (n=4M/4F) and *5xFAD;CD33*$^{-/-}$*;TREM2*$^{-/-}$ (n=5M/6F) mice. Numbers of cortical layer 5 NeuN^{+} cells were significantly increased in *5xFAD;CD33*$^{-/-}$ mice compared to *5xFAD*, *5xFAD;TREM2*$^{-/-}$ and *5xFAD;CD33*$^{-/-}$*;TREM2*$^{-/-}$ mice (*p<0.05, ***p<0.001, ****p<0.0001, one-way ANOVA, Tukey's test). Data are represented as mean ± SEM.

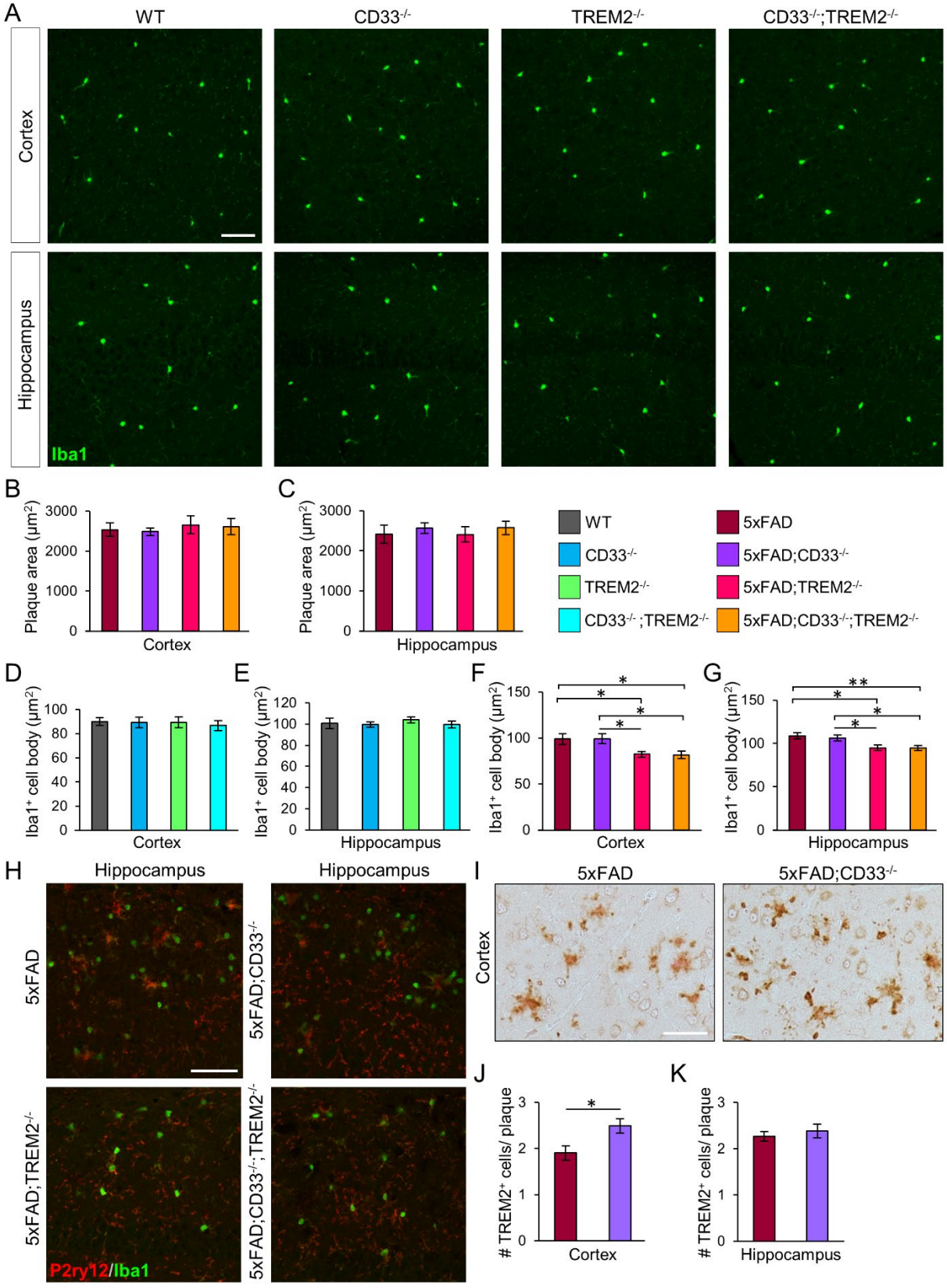
A
WT
CD33-/-
TREM2-/-
CD33-/-;TREM2-/-
Cortex
Hippocampus
Iba1
B
Plaque area (µm2)
3000
2000
1000
0
Cortex
C
Plaque area (µm2)
3000
2000
1000
0
Hippocampus
WT
CD33-/-
TREM2-/-
CD33-/-;TREM2-/-
5xFAD
5xFAD;CD33-/-
5xFAD;TREM2-/-
5xFAD;CD33-/-;TREM2-/-
D
Iba1+ cell body (µm2)
100
80
60
40
20
0
Cortex
E
Iba1+ cell body (µm2)
120
100
80
60
40
20
0
Hippocampus
F
Iba1+ cell body (µm2)
150
100
50
0
Cortex
G
Iba1+ cell body (µm2)
150
100
50
0
Hippocampus
H
Hippocampus
Hippocampus
5xFAD
5xFAD;CD33-/-
5xFAD;TREM2-/-
5xFAD;CD33-/-;TREM2-/-
P2ry12/Iba1
I
5xFAD
5xFAD;CD33-/-
Cortex
J
TREM2+ cells/ plaque
3
2
1
0
Cortex
K
TREM2+ cells/ plaque
3
2
1
0
Hippocampus

Figure S4. *CD33* and/or *TREM2* knock-out do not impact Iba1$^+$ cell body area in WT mice, Related to Figure 4. (A) Representative images from the cortex and hippocampus of 8-month-old WT, *CD33*$^{-/-}$, *TREM2*$^{-/-}$ and *CD33*$^{-/-}$*;TREM2*$^{-/-}$ mice, labeled with an Iba1-specific antibody. Scale bar represents 50 μm. (B and C) Quantification of 3D6$^+$ area of Aβ plaques in the cortex (B) and hippocampus (C) of *5xFAD* (n=7M/7F), *5xFAD;CD33*$^{-/-}$ (n=7M/7F), *5xFAD;TREM2*$^{-/-}$ (n=4M/4F) and *5xFAD;CD33*$^{-/-}$*;TREM2*$^{-/-}$ (n=5M/6F) mice at 8 months of age. Amyloid plaques that were selected for the analysis of clustering of Iba1$^+$ cells around plaques were of similar size across mouse genotypes (one-way ANOVA, Tukey's test). (D and E) Quantification of Iba1$^+$ cell body area in the cortex (D) and hippocampus (E) of 8-month-old WT (n=4M/4F), *CD33*$^{-/-}$ (n=4M/4F), *TREM2*$^{-/-}$ (n=4M/4F) and *CD33*$^{-/-}$*;TREM2*$^{-/-}$ (n=4M/4F) mice is summarized. All controls exhibited comparable Iba1$^+$ cell body area in cortex and hippocampus (one-way ANOVA, Tukey's test). (F and G) Plaque-associated Iba1$^+$ cells were analyzed for cell body area in the cortex (F) and hippocampus (G) of 8-month-old *5xFAD* (n=7M/7F), *5xFAD;CD33*$^{-/-}$ (n=7M/7F), *5xFAD;TREM2*$^{-/-}$ (n=4M/4F) and *5xFAD;CD33*$^{-/-}$*;TREM2*$^{-/-}$ (n=5M/6F) mice. *5xFAD;TREM2*$^{-/-}$ and *5xFAD;CD33*$^{-/-}$*;TREM2*$^{-/-}$ mice exhibited reduced Iba1$^+$ cell body area compared to *5xFAD* and *5xFAD;CD33*$^{-/-}$ (*p<0.05, **p<0.01, one-way ANOVA, Tukey's test). (H) Representative images from the hippocampus of 8-month-old *5xFAD*, *5xFAD;CD33*$^{-/-}$, *5xFAD;TREM2*$^{-/-}$ and *5xFAD;CD33*$^{-/-}$*;TREM2*$^{-/-}$ mice, stained with P2ry12 (red) and Iba1-specific antibody (green). Scale bar represents 50 μm. (I) Representative images of cortical fields from brains of *5xFAD* and *5xFAD;CD33*$^{-/-}$ mice, stained with an anti-TREM2 antibody and Congo red. Scale bar represents 50 μm. (J and K) The number of TREM2$^+$ cells around plaques was increased in the cortex (J) but not hippocampus (K) of 8-month-old *5xFAD;CD33*$^{-/-}$ (n=7M/7F) versus *5xFAD* (n=7M/7F) mice (*p<0.05, unpaired t-test with Welch's correction). Data are represented as mean ± SEM.

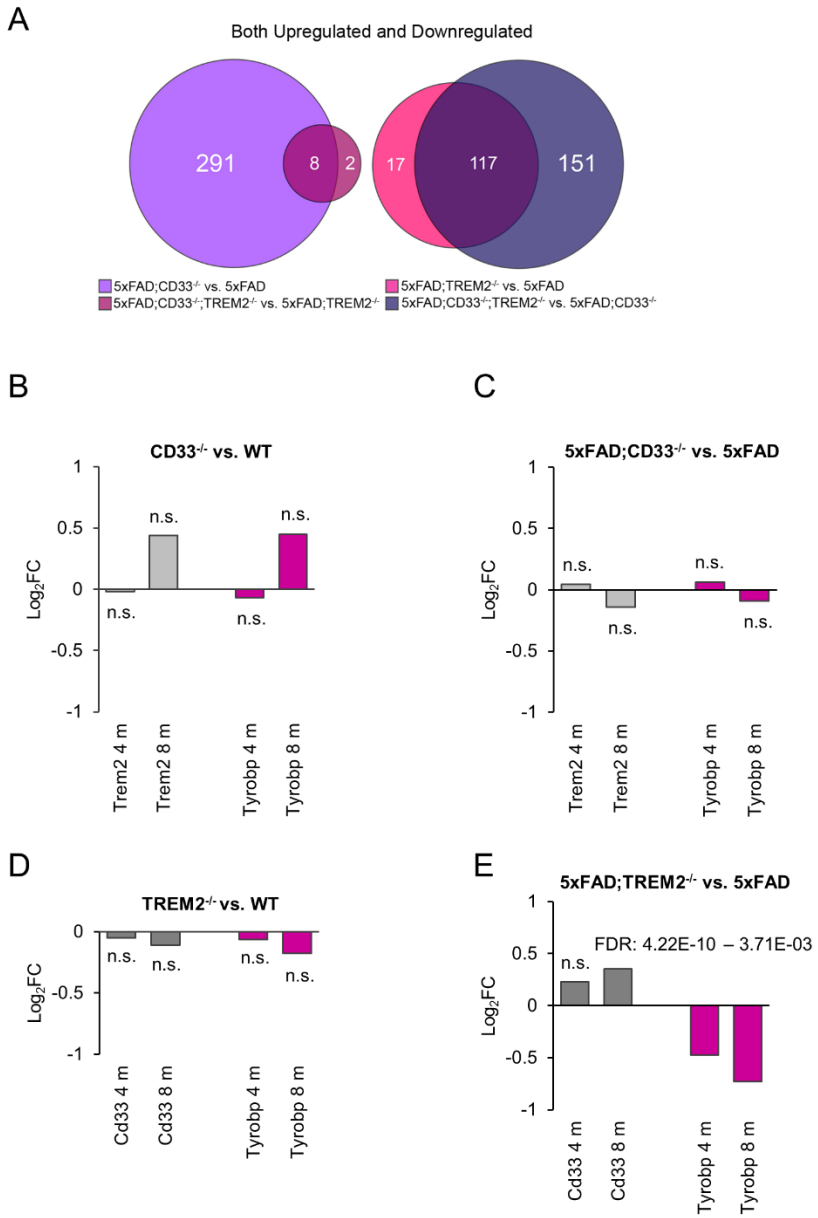

Figure S5. *CD33* and *TREM2* knock-out do not significantly impact each other's expression levels in *5xFAD* mice, while *TREM2* knock-out has a small effect on *Tyrobp* levels, Related to Figure 6. (A) Upregulated and downregulated genes (2-fold, FDR<0.05) in 4-month-old *5xFAD;CD33*$^{-/-}$ versus *5xFAD* and *5xFAD;CD33*$^{-/-}$;*TREM2*$^{-/-}$ relative to *5xFAD;TREM2*$^{-/-}$ (left), as well as in *5xFAD;TREM2*$^{-/-}$ compared to *5xFAD* and *5xFAD;CD33*$^{-/-}$;*TREM2*$^{-/-}$ versus *5xFAD;CD33*$^{-/-}$ microglia (right), displayed as Venn diagrams. *5xFAD* (n=14M/14F),

5xFAD;CD33$^{-/-}$ (n=6M/6F), *5xFAD;TREM2*$^{-/-}$ (n=11M/11F) and *5xFAD;CD33*$^{-/-}$*;TREM2*$^{-/-}$ (n=5M/5F) mice. (B-E) Expression levels of *Trem2*, *Cd33*, and *Tyrobp* were summarized as $\log_2$FC of RNA-seq carried out with microglia that were isolated from 4 and 8-month-old mice. FDR values are shown on the figure. (B and C) There was no significant change in *Trem2* or *Tyrobp* expression levels in *CD33*$^{-/-}$ versus WT (B) and *5xFAD;CD33*$^{-/-}$ versus *5xFAD* (C) datasets at 4 and 8 months. (D) *Cd33* and *Tyrobp* expression levels did not change in *TREM2*$^{-/-}$ versus WT microglia. (E) While there was no change in *Cd33* expression levels at 4 months, there was a slight increase (Log_2FC=0.35) at 8 months in the *5xFAD;TREM2*$^{-/-}$ versus *5xFAD* dataset. *Tyrobp* levels were moderately decreased at 4 months (Log_2FC=-0.47) and 8 months (Log_2FC=-0.73) in *5xFAD;TREM2*$^{-/-}$ versus *5xFAD* microglia. See also Table S3.

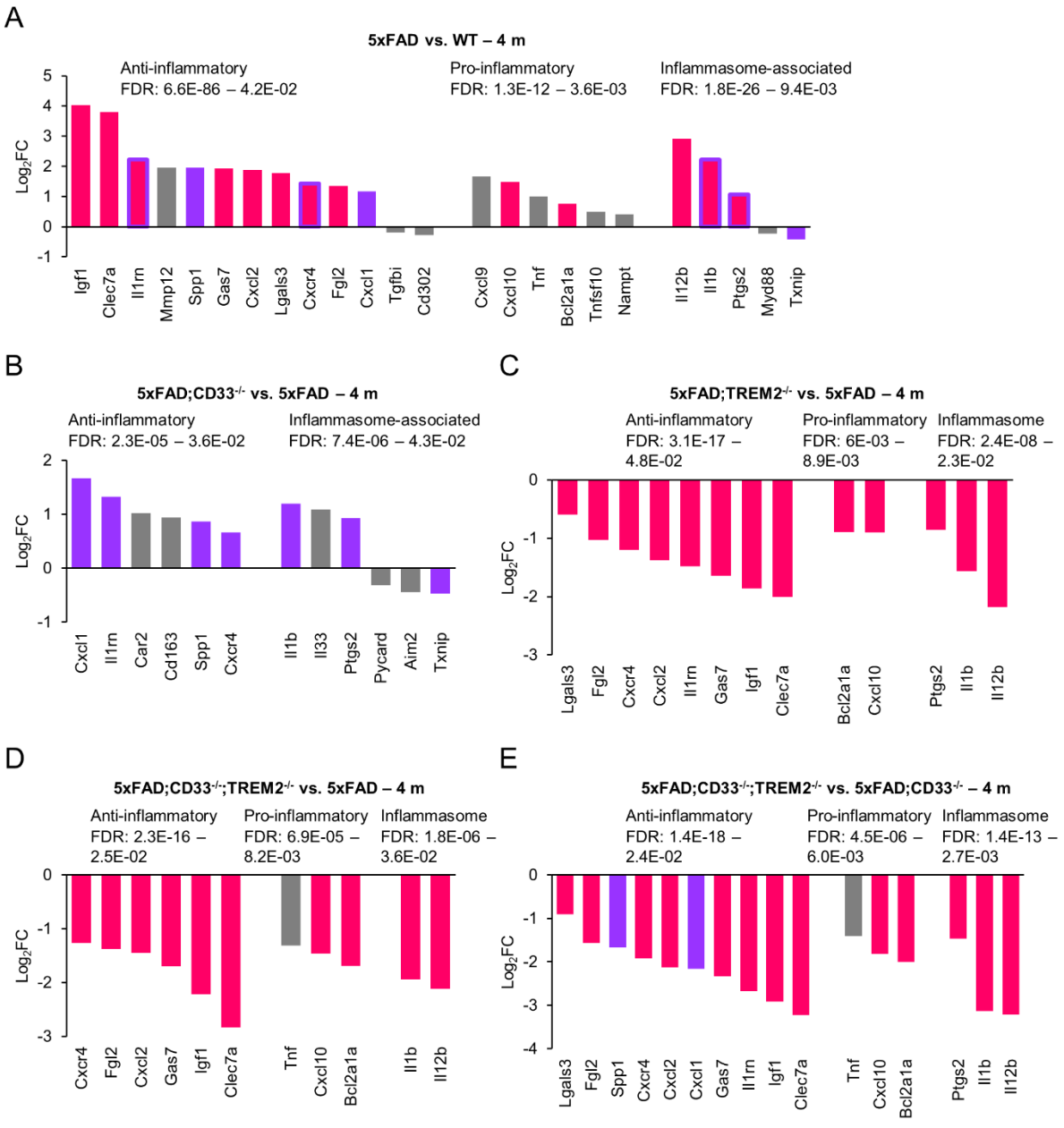
A
5xFAD vs. WT – 4 m
Anti-inflammatory
FDR: 6.6E-86 – 4.2E-02
Pro-inflammatory
FDR: 1.3E-12 – 3.6E-03
Inflammasome-associated
FDR: 1.8E-26 – 9.4E-03
Log2FC
Igf1 Clec7a Il1rn Mmp12 Spp1 Gas7 Cxcl2 Lgals3 Cxcr4 Fgl2 Cxcl1 Tgfbi Cd302 Cxcl9 Cxcl10 Tnf Bcl2a1a Tnfsf10 Nampt Il12b Il1b Ptgs2 Myd88 Txnip
B
5xFAD;CD33-/- vs. 5xFAD – 4 m
Anti-inflammatory
FDR: 2.3E-05 – 3.6E-02
Inflammasome-associated
FDR: 7.4E-06 – 4.3E-02
Log2FC
Cxcl1 Il1rn Car2 Cd163 Spp1 Cxcr4 Il1b Il33 Ptgs2 Pycard Aim2 Txnip
C
5xFAD;TREM2-/- vs. 5xFAD – 4 m
Anti-inflammatory
FDR: 3.1E-17 – 4.8E-02
Pro-inflammatory
FDR: 6E-03 – 8.9E-03
Inflammasome
FDR: 2.4E-08 – 2.3E-02
Log2FC
Lgals3 Fgl2 Cxcr4 Cxcl2 Il1rn Gas7 Igf1 Clec7a Bcl2a1a Cxcl10 Ptgs2 Il1b Il12b
D
5xFAD;CD33-/-;TREM2-/- vs. 5xFAD – 4 m
Anti-inflammatory
FDR: 2.3E-16 – 2.5E-02
Pro-inflammatory
FDR: 6.9E-05 – 8.2E-03
Inflammasome
FDR: 1.8E-06 – 3.6E-02
Log2FC
Cxcr4 Fgl2 Cxcl2 Gas7 Igf1 Clec7a Tnf Cxcl10 Bcl2a1a Il1b Il12b
E
5xFAD;CD33-/-;TREM2-/- vs. 5xFAD;CD33-/- – 4 m
Anti-inflammatory
FDR: 1.4E-18 – 2.4E-02
Pro-inflammatory
FDR: 4.5E-06 – 6.0E-03
Inflammasome
FDR: 1.4E-13 – 2.7E-03
Log2FC
Lgals3 Fgl2 Spp1 Cxcr4 Cxcl2 Cxcl1 Gas7 Il1rn Igf1 Clec7a Tnf Cxcl10 Bcl2a1a Ptgs2 Il1b Il12b

Figure S6. Downregulation of anti-inflammatory, pro-inflammatory and inflammasome-associated genes in *5xFAD;TREM2*$^{-/-}$ microglia is not reversed by additional knock-out of *CD33*, Related to Figure 6. (A-E) Expression levels of inflammation-related genes were summarized as $\log_2$FC of RNA-seq carried out with microglia from 4-month-old WT (n=13M/14F), *5xFAD* (n=14M/14F), *5xFAD;CD33*$^{-/-}$ (n=6M/6F), *5xFAD;TREM2*$^{-/-}$ (n=11M/11F) and *5xFAD;CD33*$^{-/-}$*;TREM2*$^{-/-}$ (n=5M/5F) mice. FDR values are shown on the figure. (A) Anti-inflammatory, pro-inflammatory and inflammasome-related genes were concomitantly upregulated in *5xFAD* microglia compared to WT. While pink bars in (A) overlap with (C-E), purple bars and borders overlap with (B) and (E). (B) Anti-inflammatory and inflammasome-associated genes were significantly increased in *5xFAD;CD33*$^{-/-}$ microglia versus *5xFAD*. Purple bars in (B) overlap with (A) and (E). (C) *5xFAD;TREM2*$^{-/-}$ microglia exhibited reduced expression levels of anti-inflammatory, pro-inflammatory and inflammasome-associated genes relative to *5xFAD*. Pink bars in (C) overlap with (A), (D) and (E). (D) Inflammation-related transcripts were significantly decreased in *5xFAD;CD33*$^{-/-}$*;TREM2*$^{-/-}$ microglia compared to *5xFAD.* Pink columns in (D) overlap with (A), (C) and (E). (E) Anti-inflammatory, pro-inflammatory and inflammasome-related genes were downregulated in *5xFAD;CD33*$^{-/-}$*;TREM2*$^{-/-}$ microglia versus *5xFAD;CD33*$^{-/-}$. While pink columns in (E) overlap with (A), (C) and (D), purple bars overlap with (A) and (B). See also Table S4.

A

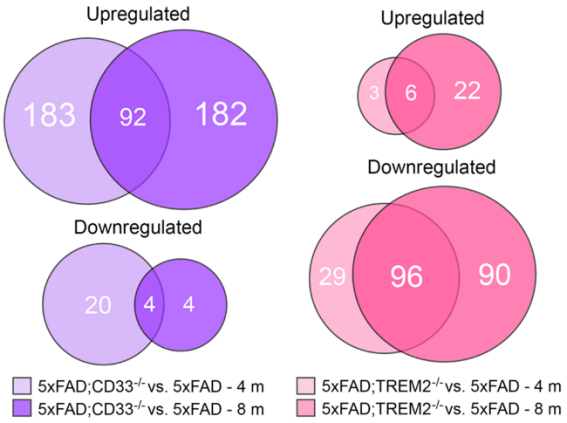
Upregulated
183
92
182
Downregulated
20
4
4
Upregulated
3
6
22
Downregulated
29
96
90
5xFAD;CD33-/- vs. 5xFAD - 4 m
5xFAD;CD33-/- vs. 5xFAD - 8 m
5xFAD;TREM2-/- vs. 5xFAD - 4 m
5xFAD;TREM2-/- vs. 5xFAD - 8 m

B

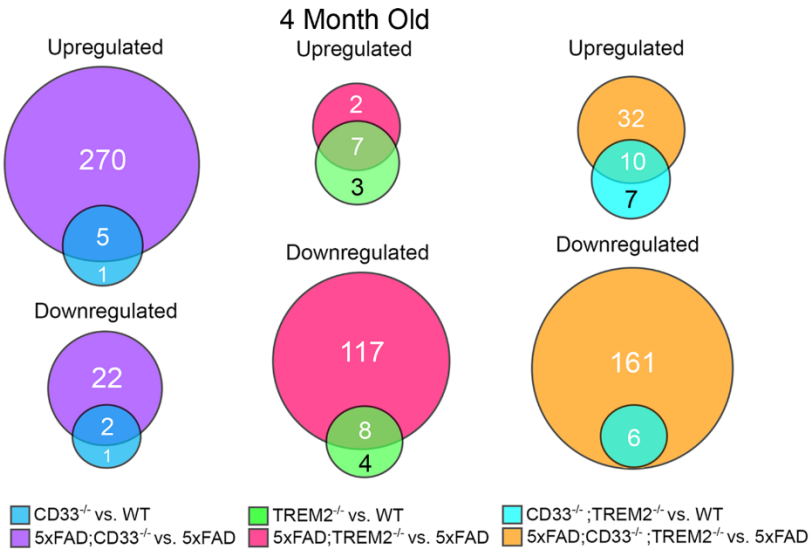
4 Month Old
Upregulated
270
5
1
Downregulated
22
2
1
Upregulated
2
7
3
Downregulated
117
8
4
Upregulated
32
10
7
Downregulated
161
6
CD33-/- vs. WT
5xFAD;CD33-/- vs. 5xFAD
TREM2-/- vs. WT
5xFAD;TREM2-/- vs. 5xFAD
CD33-/-;TREM2-/- vs. WT
5xFAD;CD33-/-;TREM2-/- vs. 5xFAD

C

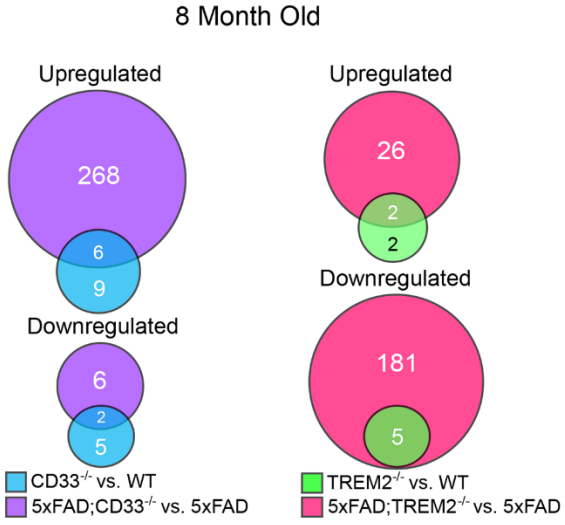
8 Month Old
Upregulated
268
6
9
Downregulated
6
2
5
Upregulated
26
2
2
Downregulated
181
5
CD33-/- vs. WT
5xFAD;CD33-/- vs. 5xFAD
TREM2-/- vs. WT
5xFAD;TREM2-/- vs. 5xFAD

Figure S7. *CD33* and/or *TREM2* knock-out lead to greater differential gene expression in *5xFAD* mice versus WT, Related to Figure 7. (A) Upregulated (top) and downregulated (bottom, 2-fold, FDR<0.05) genes in *5xFAD;CD33*$^{-/-}$ microglia compared to *5xFAD* (left) and *5xFAD;TREM2*$^{-/-}$ relative to *5xFAD* (right) at each time point, displayed as Venn diagrams. *5xFAD*: n=14M/14F, *5xFAD;CD33*$^{-/-}$: n=6M/6F at 4 months; and *5xFAD*: n=12M/12F, *5xFAD;CD33*$^{-/-}$: n=13M/13F mice at 8 months. *5xFAD*: n=14M/14F, *5xFAD;TREM2*$^{-/-}$: n=11M/11F at 4 months; and *5xFAD*: n=10M/9F, *5xFAD;TREM2*$^{-/-}$: n=9M/8F mice at 8 months. (B) Analysis of RNA-seq data revealed 9, 22 and 23 DE genes (2-fold, FDR<0.05) in *CD33*$^{-/-}$, *TREM2*$^{-/-}$ and *CD33*$^{-/-}$*;TREM2*$^{-/-}$ microglia compared to WT, respectively, at 4 months. 299, 134 and 209 genes were enriched in *5xFAD;CD33*$^{-/-}$, *5xFAD;TREM2*$^{-/-}$ and *5xFAD;CD33*$^{-/-}$*;TREM2*$^{-/-}$ microglia relative to *5xFAD*, respectively. Venn diagrams showed that 5 upregulated (top) and 2 downregulated (bottom) genes overlapped between *CD33*$^{-/-}$ microglia versus WT and *5xFAD;CD33*$^{-/-}$ versus *5xFAD* (left). 7 upregulated and 8 downregulated genes overlapped between *TREM2*$^{-/-}$ microglia versus WT and *5xFAD;TREM2*$^{-/-}$ compared to *5xFAD* (center). 10 upregulated and 6 downregulated genes overlapped between *CD33*$^{-/-}$*;TREM2*$^{-/-}$ microglia versus WT and *5xFAD;CD33*$^{-/-}$*;TREM2*$^{-/-}$ versus *5xFAD* (right). (C) At 8 months of age, 22 and 9 genes were enriched in *CD33*$^{-/-}$ and *TREM2*$^{-/-}$ microglia relative to WT, respectively, and 282 and 214 DE genes in *5xFAD;CD33*$^{-/-}$ and *5xFAD;TREM2*$^{-/-}$ microglia compared to *5xFAD*, respectively. Venn diagrams showed that 6 upregulated (top) and 2 downregulated (bottom) genes overlapped between *CD33*$^{-/-}$ microglia versus WT and *5xFAD;CD33*$^{-/-}$ relative to *5xFAD* (left). 2 upregulated and 5 downregulated genes overlapped between *TREM2*$^{-/-}$ microglia versus WT and *5xFAD;TREM2*$^{-/-}$ versus *5xFAD* (right). See also Table S6.

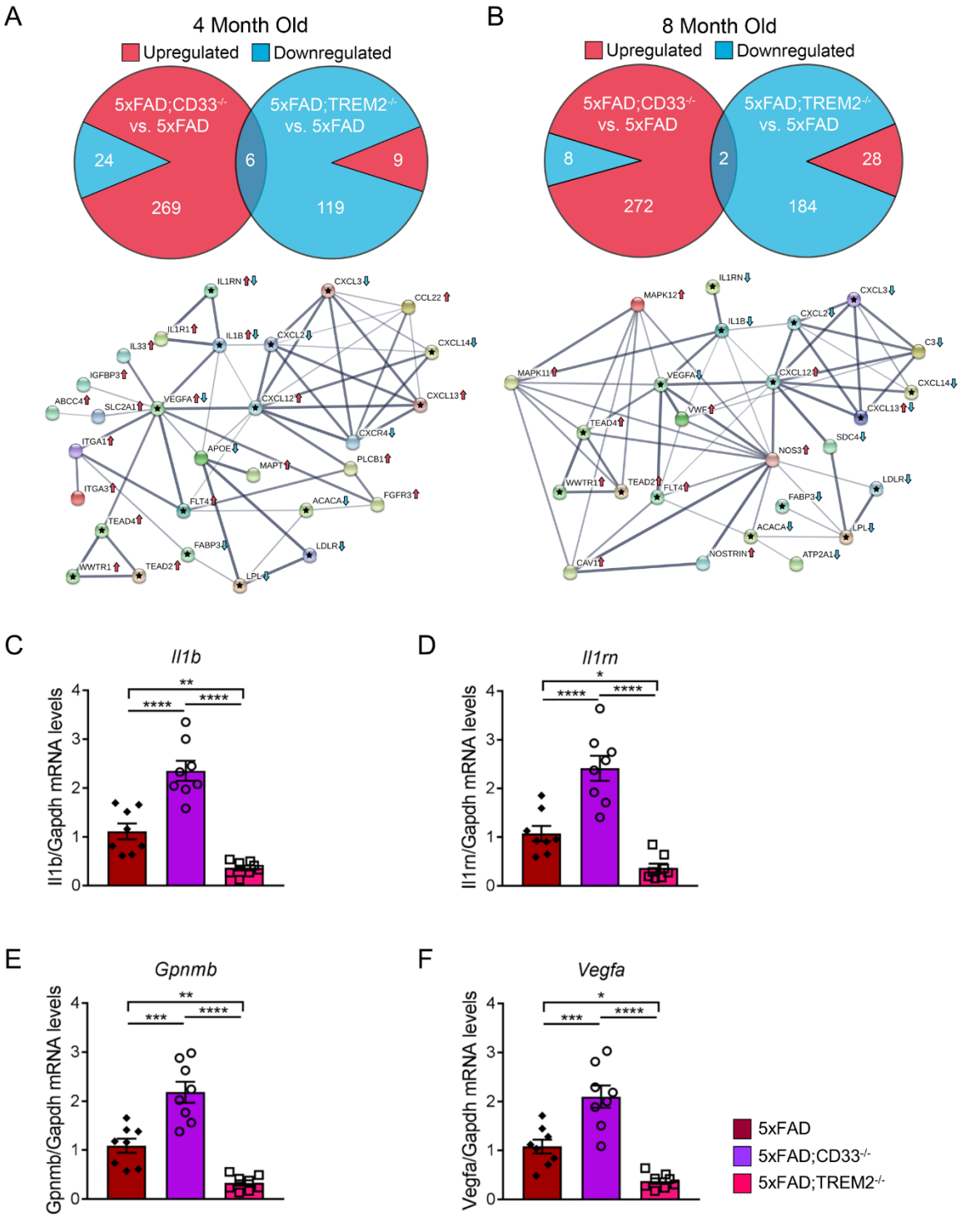
A
4 Month Old
Upregulated
Downregulated
5xFAD;CD33-/- vs. 5xFAD
5xFAD;TREM2-/- vs. 5xFAD
24
6
9
269
119
B
8 Month Old
Upregulated
Downregulated
5xFAD;CD33-/- vs. 5xFAD
5xFAD;TREM2-/- vs. 5xFAD
8
2
28
272
184
C
Il1b
Il1b/Gapdh mRNA levels
D
Il1rn
Il1rn/Gapdh mRNA levels
E
Gpnmb
Gpnmb/Gapdh mRNA levels
F
Vegfa
Vegfa/Gapdh mRNA levels
5xFAD
5xFAD;CD33-/-
5xFAD;TREM2-/-

Figure S8. IL-1β and IL-1RN are central in overlapping inflammation pathways in *5xFAD;CD33$^{-/-}$* and *5xFAD;TREM2$^{-/-}$* microglia, Related to Figure 7. (A and B) Venn diagram of pie charts showing the overlap of 6 genes (A) and 2 genes (B) that were upregulated in *5xFAD;CD33$^{-/-}$* microglia and downregulated in *5xFAD;TREM2$^{-/-}$* (versus *5xFAD*) at 4 months (A) and 8 months (B). STRING networks showed protein-protein interactions of DE genes associated with inflammation pathways that overlapped between *5xFAD;CD33$^{-/-}$* and *5xFAD;TREM2$^{-/-}$* microglia (compared to *5xFAD*) at 4 months (A) and 8 months (B). Proteins are presented as nodes, which are connected by lines whose thickness represents the confidence level in protein interaction. While red arrows represent proteins upregulated in *5xFAD;CD33$^{-/-}$*, blue arrows mark proteins downregulated in *5xFAD;TREM2$^{-/-}$* microglia. Stars highlight 16 nodes/proteins that are enriched in either genotype and overlap at 4 and 8 months, with IL-1β and IL-1RN at the center of inflammation pathways in *5xFAD;CD33$^{-/-}$* and *5xFAD;TREM2$^{-/-}$* microglia. (C-F) Validation by qPCR of top DE genes obtained with RNAseq. The qPCR analysis was performed by using microglia that were isolated from 4-month-old *5xFAD*, *5xFAD;CD33$^{-/-}$* and *5xFAD;TREM2$^{-/-}$* mice. The qPCR analysis of transcripts including *Il1b* (C), *Il1rn* (D), *Gpnmb* (E) and *Vegfa* (F) showed that mRNA levels of these transcripts were increased in *5xFAD;CD33$^{-/-}$* and decreased in *5xFAD;TREM2$^{-/-}$* microglia versus *5xFAD* (*p<0.05, **p<0.01, ***p<0.001, ****p<0.0001, one-way ANOVA, Tukey's test). *Il1b*, *Il1rn*, *Gpnmb* and *Vegfa* mRNA levels were normalized to *Gapdh* mRNA levels. Data are represented as mean ± SEM.

4 Months	P-Value	Regulation	Z-Score
5xFAD vs. WT			
Interferon Signaling	8.32E-05	↑	2.449
Role of Pattern Recognition Receptors in Recognition of Bacteria and Viruses	2.00E-03	↑	2
Mitotic Roles of Polo-Like Kinase	2.34E-03	↑	2.236
Colorectal Cancer Metastasis Signaling	3.24E-02	↑	3
Pancreatic Adenocarcinoma Signaling	3.47E-02	↑	2
5xFAD;CD33$^{-/-}$ vs. 5xFAD			
IL-6 Signaling	1.95E-04	↑	2.828
p38 MAPK Signaling	3.47E-03	↑	2.236
Sphingosine-1-phosphate Signaling	4.27E-03	↑	2.236
PPAR Signaling	6.17E-03	↑	-2.236
NF-κB Signaling	7.24E-03	↑	2.646
Acute Phase Response Signaling	1.95E-02	↑	2.449
HIPPO Signaling	2.24E-02	↑	-2
Glioblastoma Multiforme Signaling	4.90E-02	↑	2.236
5xFAD;TREM2$^{-/-}$ vs. 5xFAD			
LXR/RXR Activation	3.16E-06	↓	N/A
LPS/IL-1 Mediated Inhibition of RXR	1.35E-04	↓	N/A
Hepatic Fibrosis	3.72E-04	↓	N/A
Atherosclerosis Signaling	4.79E-04	↓	N/A
Clathrin-mediated Endocytosis Signaling	5.62E-04	↓	N/A
5xFAD;CD33$^{-/-}$TREM2$^{-/-}$ vs. 5xFAD			
Role of Pattern Recognition Receptors in Recognition of Bacteria and Viruses	3.98E-06	↓	-2
TREM1 Signaling	1.17E-05	↓	-2.449
Activation of IRF by Cytosolic Pattern Recognition Receptors	8.13E-04	↓	-2
Dendritic Cell Maturation	1.70E-03	↓	-2.236
NF-κB Signaling	3.31E-02	↓	-2
5xFAD;CD33$^{-/-}$;TREM2$^{-/-}$ vs. 5xFAD;CD33$^{-/-}$			
TREM1 Signaling	4.90E-07	↓	-2.828
Role of Pattern Recognition Receptors in Recognition of Bacteria and Viruses	4.27E-05	↓	-2
Dendritic Cell Maturation	6.76E-05	↓	-2.828
Activation of IRF by Cytosolic Pattern Recognition Receptors	2.69E-03	↓	-2
IL-6 Signaling	6.76E-03	↓	-2.236
HMGB1 Signaling	7.94E-03	↓	-2
Production of Nitric Oxide and Reactive Oxygen Species in Macrophages	9.55E-03	↓	-2.449
PPAR Signaling	1.12E-02	↓	2
Nitric Oxide Signaling in the Cardiovascular System	2.09E-02	↓	-2
Acute Phase Response Signaling	2.14E-02	↓	-2.236
NF-κB Signaling	2.63E-02	↓	-2.236
Colorectal Cancer Metastasis Signaling	2.88E-02	↓	-2.449
IL-8 Signaling	3.72E-02	↓	-2.236

8 Months	P-Value	Regulation	Z-Score
5xFAD vs. WT			
Nitric Oxide Signaling in the Cardiovascular System	1.45E-07	↑	3.273
Colorectal Cancer Metastasis Signaling	3.55E-06	↑	5.048
Dendritic Cell Maturation	2.51E-05	↑	5.099
RhoGDI Signaling	1.10E-04	↑	-4.583
Inhibition of Angiogenesis by TSP1	1.74E-04	↑	2.236
Cardiac β-adrenergic Signaling	1.78E-04	↑	2.84
Signaling by Rho Family GTPases	2.63E-04	↑	4.811
TREM1 Signaling	2.69E-04	↑	3.207
Dopamine-DARPP32 Feedback in cAMP Signaling	2.88E-04	↑	3.71
eNOS Signaling	3.55E-04	↑	3.9
Interferon Signaling	3.55E-04	↑	2.333
Sperm Motility	3.55E-04	↑	3.5
IL-8 Signaling	3.55E-04	↑	4.796
ILK Signaling	3.55E-04	↑	3.838
Cardiac Hypertrophy Signaling	5.75E-04	↑	5.099
Ephrin Receptor Signaling	7.41E-04	↑	3.317
Thrombin Signaling	1.29E-03	↑	3.273
Glioblastoma Multiforme Signaling	1.35E-03	↑	3.578
Pancreatic Adenocarcinoma Signaling	1.45E-03	↑	3.606
Gαs Signaling	1.62E-03	↑	3.606
Relaxin Signaling	1.82E-03	↑	3.464
Phospholipase C Signaling	2.51E-03	↑	4.123
Acute Phase Response Signaling	2.88E-03	↑	3.5
Integrin Signaling	3.39E-03	↑	4.6
Agrin Interactions at Neuromuscular Junction	3.89E-03	↑	3
CXCR4 Signaling	4.37E-03	↑	3
HMGB1 Signaling	4.79E-03	↑	3.5
cAMP-mediated signaling	4.90E-03	↑	3.674
Corticotropin Releasing Hormone Signaling	5.01E-03	↑	3.606
Sphingosine-1-phosphate Signaling	5.50E-03	↑	2.84
Synaptic Long Term Depression	5.50E-03	↑	3.771
Chemokine Signaling	5.75E-03	↓	-2
Tec Kinase Signaling	6.17E-03	↑	3.873
Production of Nitric Oxide and Reactive Oxygen Species in Macrophages	6.46E-03	↑	3.411
p38 MAPK Signaling	8.13E-03	↑	3.742
Calcium Signaling	8.91E-03	↑	2.646
TGF-β Signaling	9.55E-03	↑	2.333
Actin Cytoskeleton Signaling	1.10E-02	↑	3.207
Regulation of Actin-based Motility by Rho	1.15E-02	↑	2.887
Antioxidant Action of Vitamin C	1.26E-02	↑	-3.162
IL-1 Signaling	1.35E-02	↑	3
Role of Pattern Recognition Receptors in Recognition of Bacteria and Viruses	1.41E-02	↑	2.828
Gαq Signaling	1.48E-02	↑	2.84
PPAR Signaling	1.58E-02	↑	-2.887

8 Months	P-Value	Regulation	Z-Score
5xFAD vs. WT			
IL-6 Signaling	1.66E-02	↑	3.742
Endothelin-1 Signaling	1.66E-02	↑	2.065
Activation of IRF by Cytosolic Pattern Recognition Receptors	1.70E-02	↑	2.333
Cdc42 Signaling	1.82E-02	↑	2.714
PTEN Signaling	2.04E-02	↑	-3.207
NF-κB Signaling	2.19E-02	↑	4.359
CDK5 Signaling	2.51E-02	↑	2.111
Wnt/Ca^{+} pathway	2.88E-02	↑	2.828
Cholecystokinin/Gastrin-mediated Signaling	2.88E-02	↑	3.464
Complement System	2.95E-02	↑	2.236
VEGF Signaling	3.09E-02	↑	2.887
Synaptic Long Term Potentiation	3.47E-02	↓	-2
Role of NFAT in Cardiac Hypertrophy	3.89E-02	↑	3.5
GNRH Signaling	4.27E-02	↓	-2
Th1 Pathway	4.68E-02	↑	3.464
PCP pathway	4.79E-02	↑	2.449
5xFAD;CD33$^{-/-}$ vs. 5xFAD			
Leukocyte Extravasation Signaling	4.37E-03	↑	2.236
Acute Phase Response Signaling	4.79E-03	↑	2.236
Phospholipase C Signaling	2.57E-02	↑	2
IL-8 Signaling	3.31E-02	↑	2.449
Thrombin Signaling	3.80E-02	↑	2.236
Mouse Embryonic Stem Cell Pluripotency	4.07E-02	↑	2
Corticotropin Releasing Hormone Signaling	4.68E-02	↑	2
5xFAD;TREM2$^{-/-}$ vs. 5xFAD			
Dendritic Cell Maturation	1.95E-06	↓	-3
Toll-like Receptor Signaling	2.69E-04	↓	-2
Th1 Pathway	5.75E-04	↓	-2.449
Calcium-induced T Lymphocyte Apoptosis	1.41E-03	↓	-2
iCOS-iCOSL Signaling in T Helper Cells	2.40E-03	↓	-2.236
TREM1 Signaling	2.69E-03	↓	-2
IL-6 Signaling	3.02E-03	↓	-2
PKCθ Signaling in T Lymphocytes	3.39E-03	↓	-2.236
Cholecystokinin/Gastrin-mediated Signaling	7.76E-03	↓	-2
IL-8 Signaling	1.82E-02	↓	-2.236
Acute Phase Response Signaling	4.17E-02	↓	-2

Table S2. Effects of aging and knock-out of *CD33* and/or *TREM2* on biological pathways in *5xFAD* microglia, Related to Figures 5, 6 and 7. Early (4 months of age) and late (8 months of age) downregulated and upregulated gene data sets (2-fold difference, FDR<0.05) were analyzed by Ingenuity Pathway Analysis (IPA). IPA revealed upregulation and activation of most pathways in 4-month-old *5xFAD* microglia compared to WT and in *5xFAD;CD33*$^{-/-}$ versus *5xFAD*. Most pathways were downregulated and inhibited in *5xFAD;TREM2*$^{-/-}$ microglia relative to *5xFAD*, *5xFAD;CD33*$^{-/-}$*;TREM2*$^{-/-}$ compared to *5xFAD* and *5xFAD;CD33*$^{-/-}$*;TREM2*$^{-/-}$ versus *5xFAD;CD33*$^{-/-}$ at 4 months of age. IPA analysis also showed that most pathways were upregulated and activated in 8-month-old *5xFAD* microglia relative to WT. While *CD33* knock-out led to upregulation and activation of pathways, *TREM2* knock-out resulted in downregulation and inhibition of pathways in *5xFAD* microglia at 8 months of age. Activation Z-scores were generated by IPA; Z-score<-2, pathway inhibited; Z-score>2, pathway activated; p-value<0.05. N/A: not applicable. See also Tables S1, S3 and S5.